

Atomic non-classicality: A study of the anti-Jaynes-Cummings interaction

Christopher Mayo^{*}

Tom Mboya University, Department of Physics, C19, P.O. Box 199-40300, Homabay, Kenya

(Dated: August 20, 2024)

We apply the Wigner-Yanase skew information, $I(\hat{\rho}, \hat{K})$, as a quantum information quantifier of atomic non-classicality in the dynamics generated by the anti-Jaynes-Cummings (AJC) Hamiltonian when a two-level atom in an initial atomic ground state $|g\rangle$ couples to a single mode of squeezed coherent light. We investigate the effect of variation of squeeze parameter, r , field intensity, $|\alpha|^2$, and coupling strength parameter, ξ , on the dynamics of, $I(\hat{\rho}, \hat{K})$. We observe that, $I(\hat{\rho}, \hat{K})$ records mixed state values for all variations of r , $|\alpha|^2$, ξ congruent with squeezing effects.

Keywords: anti-Jaynes-Cummings; squeezed coherent state; atomic inversion; Wigner-Yanase skew information; non-classicality.

1. INTRODUCTION

The simplest single-mode spin-boson model that describes the interaction between light and matter is the quantum Rabi model (QRM) [1–5]. This Hamiltonian has two dynamical frames [6]; the rotating frame (RF) and the counter (anti)-rotating frame (CRF). The dynamics in the rotating frame [7, 8] is governed by the Jaynes-Cummings (JC) interaction process and through a $U(1)$ symmetry transformation generated by the JC excitation number operator $\hat{N} = \hat{a}^\dagger \hat{a} + \hat{\sigma}_+ \hat{\sigma}_-$. In this case, the QRM is approximated by an effective JC Hamiltonian, \hat{H} , [5, 9–15] in the rotating wave approximation (RWA). In the RWA, the coupling strength, λ , is much weaker than the mode frequency, ω , i.e., $\lambda \ll |\omega|$. In this circumstances, if the qubit is close to resonance, $|\omega_0| - |\omega| \simeq 0$, and $|\omega_0 + \omega| \geq |\omega_0 - \omega|$ holds, the RWA can be applied. This implies neglecting terms that rotate at frequency $\omega_0 + \omega$, leading to the JC Hamiltonian. On the other hand, dynamics in the CRF, is controlled by the anti-Jaynes-Cummings (AJC) interaction process [6, 7, 16–18] through a $U(1)$ symmetry transformation generated by the AJC conserved excitation number operator, $\hat{N} = \hat{a} \hat{a}^\dagger + \hat{\sigma}_- \hat{\sigma}_+$. The QRM in this sense is approximated by an effective AJC Hamiltonian, \hat{H} , in the counter-rotating wave approximation (CRWA) in the form $|\omega_0 - \omega| \geq |\omega_0 + \omega|$. Here, terms that rotate at frequencies $\omega_0 - \omega$ are dropped resulting to the AJC Hamiltonian, \hat{H} . The AJC model, \hat{H} , as a component of the QRM in the CRF, is exactly solvable [6] and features a conserved excitation number operator. Recently, It has been demonstrated [7, 8] that it is feasible to generate entangled anti-symmetric atom-field states, entangled symmetric atom-field states in the AJC, JC processes respectively while in [17, 18] non-classicality in the AJC process as measured by the Mandel-Q parameter is discussed. During the AJC interaction [7], the Rabi oscillations occur in the reverse sense in relation to that during the JC interaction mechanism.

In this article, we study atomic non-classicality dynamics generated by the AJC Hamiltonian when a two-level atom interacts with a quantised field mode initially in a squeezed state [13, 19–28], measured by the Weigner-Yanase skew information [29].

The Wigner-Yanase skew information [29]

$$I(\hat{\rho}, \hat{K}) = -\frac{1}{2} \text{tr} \left[\sqrt{\hat{\rho}} \hat{K} \right]$$

is a measure of the information content of a pure state or a mixed state, $\hat{\rho}$, skew to an observable (Hermitian operator), \hat{K} , where $[,]$ denotes the commutator. In the following, without loss of generality, we shall interpret the time evolution of the Wigner-Yanase skew information based on the simplified redefinition in [30] christened atomic spin non-classicality quantifier in the form

$$N(\hat{\rho}) = \frac{1}{2} \left(1 - \sqrt{1 - |\vec{r}|^2} \right)$$

* E-mail address: cmayero@tmu.ac.ke

where $\vec{r} = r_x \hat{i} + r_y \hat{j} + r_z \hat{k}$ is the Bloch vector. It therefore follows that; when $|\vec{r}| = 0$, $N(\hat{\rho}) = 0$ corresponds to a maximally mixed (maximally entangled) state, $|\vec{r}| = 1$, $N(\hat{\rho}) = \frac{1}{2}$ pure (product) state else $0 < |\vec{r}| < 1$, $0 < N(\hat{\rho}) < \frac{1}{2}$, mixed (entangled) state.

It has been established in [17, 18] that a non-vanishing residual detuning, 2ω , exists in the AJC process and absent in the standard JC resonance, $\delta = 0$. This being a fundamental distinctive internal dynamical property of the AJC interaction mechanism, a residual detuning parameter, $\xi = \frac{\omega}{\lambda}$ present in the general definition of sum frequency, $\bar{\delta} = 2\xi\lambda$ at $\delta = 0$ is interpreted as a coupling strength, where ω , λ are field mode frequency, coupling constant respectively. Small values of ξ such that $\lambda \gg \omega$ signifies strong atom-field AJC interaction. We study the effect of the coupling strength parameter on the dynamics of Wigner-Yanase skew information during the atom-field AJC interaction process in addition to effects arising from variation of field intensity, $|\alpha|^2$ and squeeze parameter, r .

This work is organised as follows; Sec. 2 introduces the AJC theoretical model and its time evolution; in Sec. 3 non-classicality as measured by the Weigner-Yanase skew information is provided and Sec. 4 is the conclusion.

2. THE AJC MODEL AND ITS TIME EVOLUTION

The AJC Hamiltonian as a component of the QRM in the CRF determined in anti-normal order form is defined as

$$\hat{H} = \hbar \left[\omega \hat{N} + \bar{\delta} \hat{s}_z + \lambda (\hat{a} \hat{s}_- + \hat{a}^\dagger \hat{s}_+) - \frac{1}{2} \omega \right] \quad ; \quad \hat{N} = \hat{a} \hat{a}^\dagger + \hat{s}_- \hat{s}_+ \quad ; \quad \bar{\delta} = \omega_0 + \omega \quad ; \quad \lambda = 2g. \quad (1)$$

Here, ω is the field mode frequency; ω_0 is the atomic transition frequency; g is the atom-field coupling constant; \hat{a} , \hat{a}^\dagger are the field annihilation and creation operators, respectively obeying $[\hat{a}, \hat{a}^\dagger] = 1$; \hat{s}_z is the atomic inversion operator; and $\hat{s}_+ = \hat{s}_x + i\hat{s}_y$, $\hat{s}_- = \hat{s}_x - i\hat{s}_y$ are the atomic transition operators and satisfy $[\hat{s}_+, \hat{s}_-] = 2\hat{s}_z$, $[\hat{s}_z, \hat{s}_\pm] = \pm\hat{s}_\pm$ with $\hat{s}_x = \frac{1}{2}\hat{\sigma}_x$, $\hat{s}_y = \frac{1}{2}\hat{\sigma}_y$, $\hat{s}_z = \frac{1}{2}\hat{\sigma}_z$ the well-known Pauli spin operator matrices. The operator, \hat{N} , is the AJC conserved excitation number operator.

We express the AJC sum frequency detuning, $\bar{\delta} = \omega_0 + \omega$, in Eq. (1) in terms of the JC difference frequency detuning, $\delta = \omega_0 - \omega$, in the form

$$\bar{\delta} = \delta + 2\omega \quad (2)$$

to conveniently vary δ , AJC residual detuning, 2ω , separately during analysis of atomic non-classicality dynamics generated by the AJC Hamiltonian defined in Eq. (1). With reference to Eq.(2), notice that when $\delta = 0$, $\bar{\delta} = 2\omega$ is a non-vanishing residual frequency detuning observed only in the AJC process and defined earlier in [31–33] as the Bloch-Siegert oscillation (BSO).

In this work, we consider an atom initially in an atomic ground state $|g\rangle$ and the field mode initially in a squeezed coherent state $|\alpha, r\rangle_{t=0}$ defined as [13]

$$\begin{aligned} |\alpha, r\rangle_{t=0} &= S_n |n\rangle \quad ; \\ S_n &= \frac{1}{\sqrt{\cosh(r)}} \exp \left[-\frac{1}{2} |\alpha|^2 - \frac{1}{2} \alpha^{*2} \tanh(r) \right] \\ &\times \sum_{n=0}^{\infty} \frac{\left[\frac{1}{2} \tanh(r) \right]^{\frac{n}{2}}}{\sqrt{n!}} \times H_n \left[(\alpha \cosh(r) + \alpha^* \sinh(r)) (\sinh(2r))^{-\frac{1}{2}} \right] \quad ; \quad \theta = 0 \end{aligned} \quad (3)$$

where α is the coherent state mean photon number amplitude, r is the squeeze parameter and S_n is the probability amplitude for n -photons in the state $|n\rangle$, giving the probability of finding n photons in the field in the form [13]

$$\begin{aligned} P(n) &= |S_n|^2 = |\langle n | \alpha, r \rangle|^2 \\ &= \frac{\left[\frac{1}{2} \tanh(r) \right]^n}{n! \cosh(r)} \exp \left[-|\alpha|^2 - \frac{1}{2} (\alpha^{*2} + \alpha^2) \tanh(r) \right] \\ &\times \left| H_n \left[(\alpha \cosh(r) + \alpha^* \sinh(r)) (\sinh(2r))^{-\frac{1}{2}} \right] \right|^2. \end{aligned} \quad (4)$$

The initial average photon number, $\langle \hat{n} \rangle$, of a squeezed coherent state is a sum of the coherent and the squeeze contributions, which in this respect

$$\langle \hat{n} \rangle = |\alpha|^2 + \sinh^2(r) \quad ; \quad |\alpha|^2 = \langle \hat{a}\hat{a}^\dagger \rangle_{t=0} = \langle \hat{a}^\dagger \hat{a} + 1 \rangle_{t=0}. \quad (5)$$

The composite atom-field mode initial state $|\psi_{g\alpha}\rangle$ takes the form [34]

$$|\psi_{g\alpha}\rangle = |g\rangle \otimes |\alpha, r\rangle = \sum_{n=0}^{\infty} S_n |g, n\rangle. \quad (6)$$

Acting on this initial state, Eq. (6), the AJC Hamiltonian in Eq. (1), generates a time evolving state vector, $|\bar{\Psi}_{g\alpha}(t)\rangle$, expressed in Schmidt decomposition [13, 35, 36] form

$$\begin{aligned} |\bar{\Psi}_{g\alpha}(t)\rangle &= e^{-\frac{i}{\hbar}\hat{H}t} |\psi_{g\alpha}\rangle = \sum_{n=0}^{\infty} \left[e^{-i\omega(n+1)t} S_n \left(\cos(\bar{R}_{gn}t) \right. \right. \\ &\quad \left. \left. + i\bar{c}_{gn} \sin(\bar{R}_{gn}t) \right) |g\rangle - i e^{-i\omega n t} S_{n-1} \bar{s}_{gn-1} \sin(\bar{R}_{gn-1}t) |e\rangle \right] \otimes |n\rangle ; \\ \bar{R}_{gn} &= \frac{\lambda}{2} \sqrt{4n+4 + (\beta+2\xi)^2} \quad ; \quad \bar{c}_{gn} = \frac{(\beta+2\xi)}{\sqrt{4n+4 + (\beta+2\xi)^2}} \\ \bar{s}_{gn} &= \sqrt{\frac{4(n+1)}{4n+4 + (\beta+2\xi)^2}} \quad ; \quad \bar{\delta} = (\beta+2\xi)\lambda \quad ; \quad \xi = \frac{\omega}{\lambda} \quad ; \quad \beta = \frac{\delta}{\lambda}. \end{aligned} \quad (7)$$

In Eq. (7), $\beta = \frac{\delta}{\lambda}$, $\xi = \frac{\omega}{\lambda}$ are dimensionless detuning parameters, with ξ a non-vanishing dimensionless frequency detuning parameter interpreted as a coupling strength such that small values of ξ in the range (0, 1) specify a strongly coupled atom-field system in the AJC interaction and large values of ξ greater than unity characterises a weakly coupled atom-field quantum system in AJC process.

3. DYNAMICS OF ATOMIC NON-CLASSICALITY

In this section we apply the Wigner-Yanase skew information [29] as a measure of the information content of the time-evolving reduced density operator of the atom $\hat{\rho}_a^g(t)$ skew to a Hermitian operator, \hat{s}_z , in the form

$$I\left(\hat{\rho}_a^g(t), \hat{s}_z\right) = -\frac{1}{2} \text{tr} \left[\sqrt{\hat{\rho}_a^g(t)}, \hat{s}_z \right]^2 \quad ; \quad \hat{K} = \hat{s}_z. \quad (8a)$$

The skew information in Eq. (8a), constitutes an alternative measure for the information content of the time-evolving state $\hat{\rho}_a^g(t)$ skew to the observable, \hat{s}_z , which based on the redefinition in [30] we write in the case of pure states (product states), $I(\cdot) = \frac{1}{2}$, mixed states (entangled states), $0 < I(\cdot) < \frac{1}{2}$, and maximally mixed states (maximally entangled states), $I(\cdot) = 0$.

The time-evolving reduced density operator of the atom $\hat{\rho}_a^g(t)$ in Eq. (8a) is easily obtained by tracing [13, 36–39] the time evolving AJC density matrix $\hat{\rho}_{g\alpha}(t)$ over the field mode states, determined from Eq. (7) according to

$$\begin{aligned} \hat{\rho}_a^g(t) &= \text{tr}_f \hat{\rho}_{g\alpha} = \text{tr}_f (|\bar{\Psi}_{g\alpha}(t)\rangle \langle \bar{\Psi}_{g\alpha}(t)|) \\ &= \sum_{n=0}^{\infty} \left[S_n^2 \left(\cos^2(\bar{R}_{gn}t) + \bar{c}_{gn}^2 \sin^2(\bar{R}_{gn}t) \right) |g\rangle \langle g| \right. \\ &\quad \left. + i S_n S_{n-1} \bar{s}_{gn-1} e^{-i\omega t} \sin(\bar{R}_{gn-1}t) \left(\cos(\bar{R}_{gn}t) + i\bar{c}_{gn} \sin(\bar{R}_{gn}t) \right) |g\rangle \langle e| \right. \\ &\quad \left. - i S_n S_{n-1} \bar{s}_{gn-1} e^{i\omega t} \sin(\bar{R}_{gn-1}t) \left(\cos(\bar{R}_{gn}t) - i\bar{c}_{gn} \sin(\bar{R}_{gn}t) \right) |e\rangle \langle g| \right. \\ &\quad \left. + S_{n-1}^2 \bar{s}_{gn-1}^2 \sin^2(\bar{R}_{gn-1}t) |e\rangle \langle e| \right]. \end{aligned} \quad (8b)$$

With reference to Eq. (2), at the standard resonance condition, $\delta = 0$, i.e., $\omega_0 = \omega$, the AJC Rabi frequency, \bar{R}_{gn} and interaction parameters \bar{c}_{gn} , \bar{s}_{gn} in Eq. (7) take the forms

$$\bar{R}_{gn} = \lambda \sqrt{n+1 + \xi^2} \quad ; \quad \bar{c}_{gn} = \frac{\xi}{\sqrt{n+1 + \xi^2}} \quad ; \quad \bar{s}_{gn} = \frac{\sqrt{n+1}}{\sqrt{n+1 + \xi^2}}, \quad (9)$$

confirming the explicit dependence of $\bar{R}_{gn}, \bar{c}_{gn}, \bar{s}_{gn}$ on ξ .

It therefore follows from Eq.(9), zero difference frequency detuning, $\delta = 0$, and consequently sum frequency, $\bar{\delta} = 2\omega = 2\xi\lambda$, will provide a clear picture of the effect of coupling strength, ξ , during the AJC atom-field interaction measured by the Wigner-Yanase skew information, $I(\hat{\rho}_a^g(t), \hat{s}_z)$. In the following, incipiently Sec. 3.1, we evaluate the Wigner-Yanase skew information, $I(\hat{\rho}_a^g(t), \hat{s}_z)$, defined in Eq. (8a), specifically at $\delta = 0$; $\bar{\delta} = 2\xi\lambda$, for different values of coupling strength, ξ and provide the corresponding $I(\cdot)$ dynamical evolution curves.

It is also important to recall that when an ideal two-level atom interacts with a quantised optical field, the result is quantum collapses and revivals in atomic population inversion [10, 11, 13, 17, 18, 25, 34, 40], where the revivals are an indicator of the nature of photon number distribution $P(n)$ Eq. (4) of the initial field mode inside a cavity. In this article, to have a clear visual of the non-classical nature of the AJC atom-field interaction measured by $I(\hat{\rho}_a^g(t), \hat{s}_z)$, we introduce atomic population inversion, $W(t)$, defined as the difference of time-evolving excited state probability, $\bar{P}_e(t)$, and time-evolving ground state probability, $\bar{P}_g(t)$, according to

$$W(t) = \bar{P}_e(t) - \bar{P}_g(t), \quad (10a)$$

which in terms of the time-evolving reduced density matrix of the atom, $\hat{\rho}_a^g(t)$, explicitly defined in Eq. (8b), we write

$$\begin{aligned} W(t) &= \text{tr}(\hat{\sigma}_z \hat{\rho}_a^g(t)), \\ &= \sum_{n=0}^{\infty} [S_{n-1}^2 \bar{s}_{gn-1}^2 \sin^2(\bar{R}_{gn-1}t) - S_n^2 (\cos^2(\bar{R}_{gn}t) + \bar{c}_{gn}^2 \sin^2(\bar{R}_{gn}t))] . \end{aligned} \quad (10b)$$

We use this expression in Eq. (10b), to evaluate $W(t)$ and compare with that determined for $I(\hat{\rho}_a^g(t), \hat{s}_z)$ at equal values of field intensity, $|\alpha|^2$, squeeze parameter, r , and coupling strength ξ in Sec. 3.1.

Further investigation on the dynamics of $I(\cdot)$ during the AJC process set at AJC resonance condition $\bar{\delta} = 2\xi\lambda$; $\delta = 0$ while varying field intensity, $|\alpha|^2$, and squeeze parameter, r , is provided in Secs. 3.2, 3.3 respectively.

3.1. Variation of coupling strength

The coupling strength parameter, ξ , is the ratio of the field mode frequency to coupling constant, $\omega : \lambda$, and it is a dimensionless quantity since ω, λ are defined in units of frequency, s^{-1} . We set field intensity, squeeze parameter, at arbitrary constant values of $|\alpha|^2 = 30$, $r = 2$ and vary the coupling strength parameter, $\xi = 0.0001, 0.01, 1.5, 2$ in the plots of time evolution of the Wigner-Yanase skew information $I(\hat{\rho}_a^g(\tau), \hat{s}_z)$ in Figs. (1a), (1b), (1c), (1d) at $\beta = \frac{\delta}{\lambda} = 0$, ($\delta = 0$). Fig. (1a), provides an additional plot of time evolution of atomic population inversion, $W(\tau)$ set at the same, $|\alpha|^2, r, \beta$ parameter values. In $I(\hat{\rho}_a^g(\tau), \hat{s}_z)$, $W(\tau)$, the temporal parameter, $\tau = \lambda t$ is the scaled time.

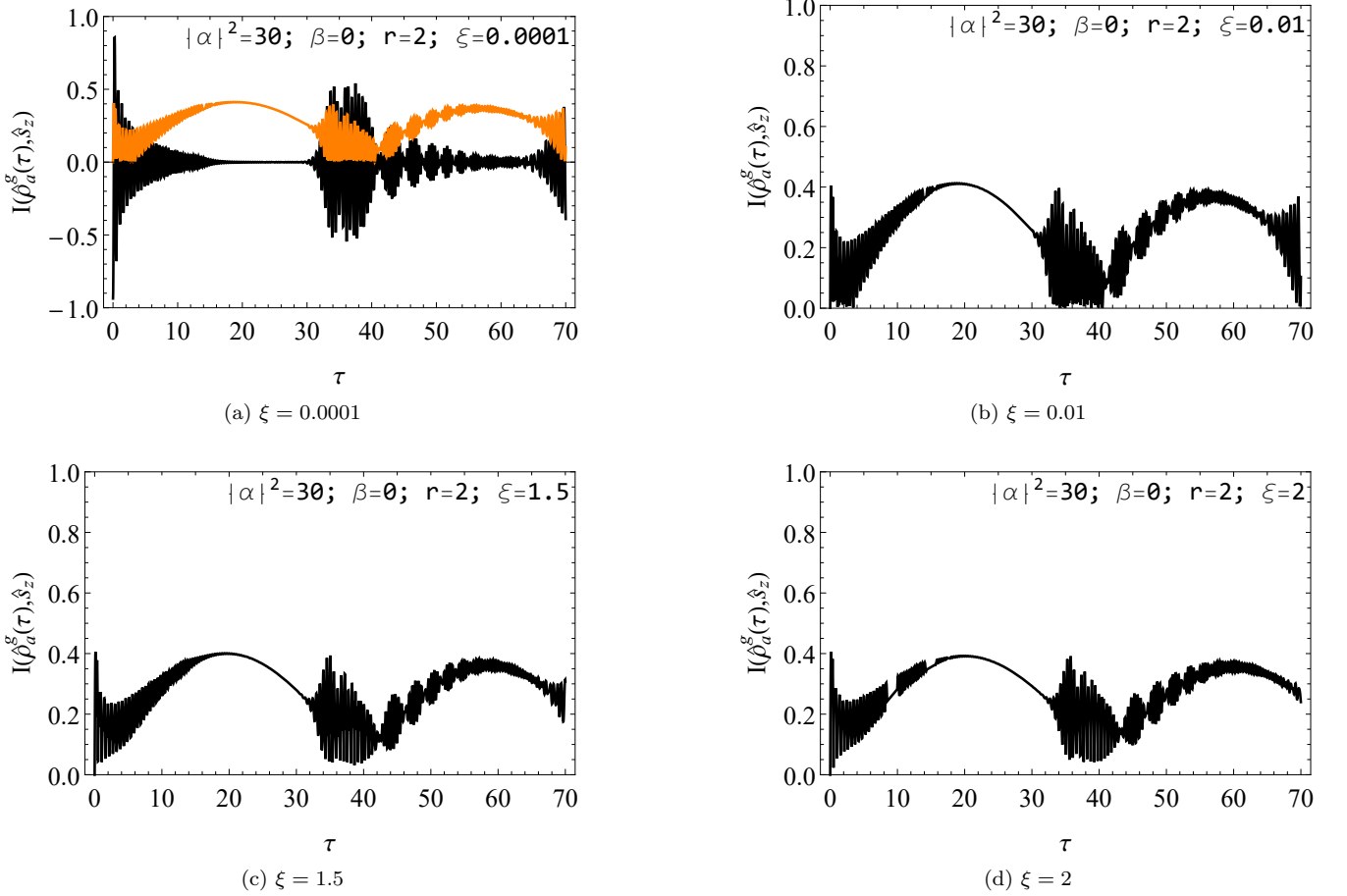


FIG. 1: Time evolution of Wigner-Yanase Skew Information $I(\hat{\rho}_a^g(t), \hat{s}_z)$ at $\bar{\delta} = 2\xi\lambda$ ($\beta = 0, \delta = 0$), $r = 2$, $|\alpha|^2 = 30$: Fig. (1a), $W(\tau)$ (black); $I(\cdot)$ (orange) at $\bar{\delta} = 0.0002\lambda$, $\xi = 0.0001$, Fig. (1b), $\bar{\delta} = 0.02\lambda$, $\xi = 0.01$, Fig. (1c), $\bar{\delta} = 3\lambda$, $\xi = 1.5$ and Fig. (1d) $\bar{\delta} = 4\lambda$, $\xi = 2$.

In the plots in Fig. 1 we see that:

- (i) at the middle of collapse of atomic population inversion in Fig. 1a, the system evolves to a low degree of mixedness, $I(\cdot) = 0.4$, slightly below a pure state limit of $I(\cdot) = 0.5$ and later evolves into a state of maximal mixedness, $I(\cdot) = 0$, periodically similar to the collapse time, $\tau_c = \frac{1}{\sqrt{2}}$, in $I(\cdot)$, $W(\tau)$ as a consequence of strongly coupled AJC atom-field interaction set at $\xi = 0.0001$;
- (ii) ringing revivals in $W(\tau)$, $I(\cdot)$ are present in all plots in Fig. 1. This is as a consequence of overlapping of additional peaks in the photon number distribution $P(n)$ Eq. (4) for all $r > 1$, see [18, 23, 25, 41]. The additional peaks in the photon counting distribution are a result of an increased addition of squeezed photons in the coherent field mode, discussed earlier in [18, 23, 25, 41];
- (iii) Fig. 1b displays a similar form of time evolution of the Wigner-Yanase skew information, $I(\cdot)$, to that presented in Fig. 1a, however notice a slight lift in $I(\cdot)$ at all time intervals above the maximally mixed state value, $I(\cdot) = 0$, as a result of the reduced coupling, $\xi = 0.01$. This can be visualised more clearly on Figs. 1c, 1d where at respective weak coupling, $\xi = 1.5, 2$, the time evolution of $I(\cdot)$ is strictly mixed away from maximal mixedness $I(\cdot) = 0$;
- (iv) an decrease in the coupling strength from $\xi = 0.01$ in Fig. 1b to $\xi = 1.5$ in Fig. 1c and finally to $\xi = 2$ in Fig. 1d, results in delay in revivals leading to longer quiescent phases in the evolution of $I(\cdot)$ and;
- (v) despite reduction in coupling strength parameter, $\xi \gg 0.0001$, resulting into longer collapse period in $I(\cdot)$ Figs. 1c, 1d, the atom-field system is maintained in a mixed state range, $0 < I(\cdot) < 0.5$, at all time intervals as expected when an initial squeezed field-mode state is considered [18, 23].

3.2. Variation of field intensity

In this section we investigate the effect of field intensity, $|\alpha|^2$, on the dynamics of the Wigner-Yanase skew information, $I(\hat{\rho}_a^g(\tau), \hat{s}_z)$, while keeping difference frequency detuning, δ , squeeze parameter, r , coupling strength parameter, ξ , fixed at $\delta = \omega_0 - \omega = 0$; $\beta = 0$, $r = 1.5$, $\xi = 0.9$. We arbitrarily set the field intensity at, $|\alpha|^2 = 10, 20, 30, 40$, and provide the $I(\cdot)$ dynamical evolution plots in Figs. 2a, 2b, 2c and 2d respectively.

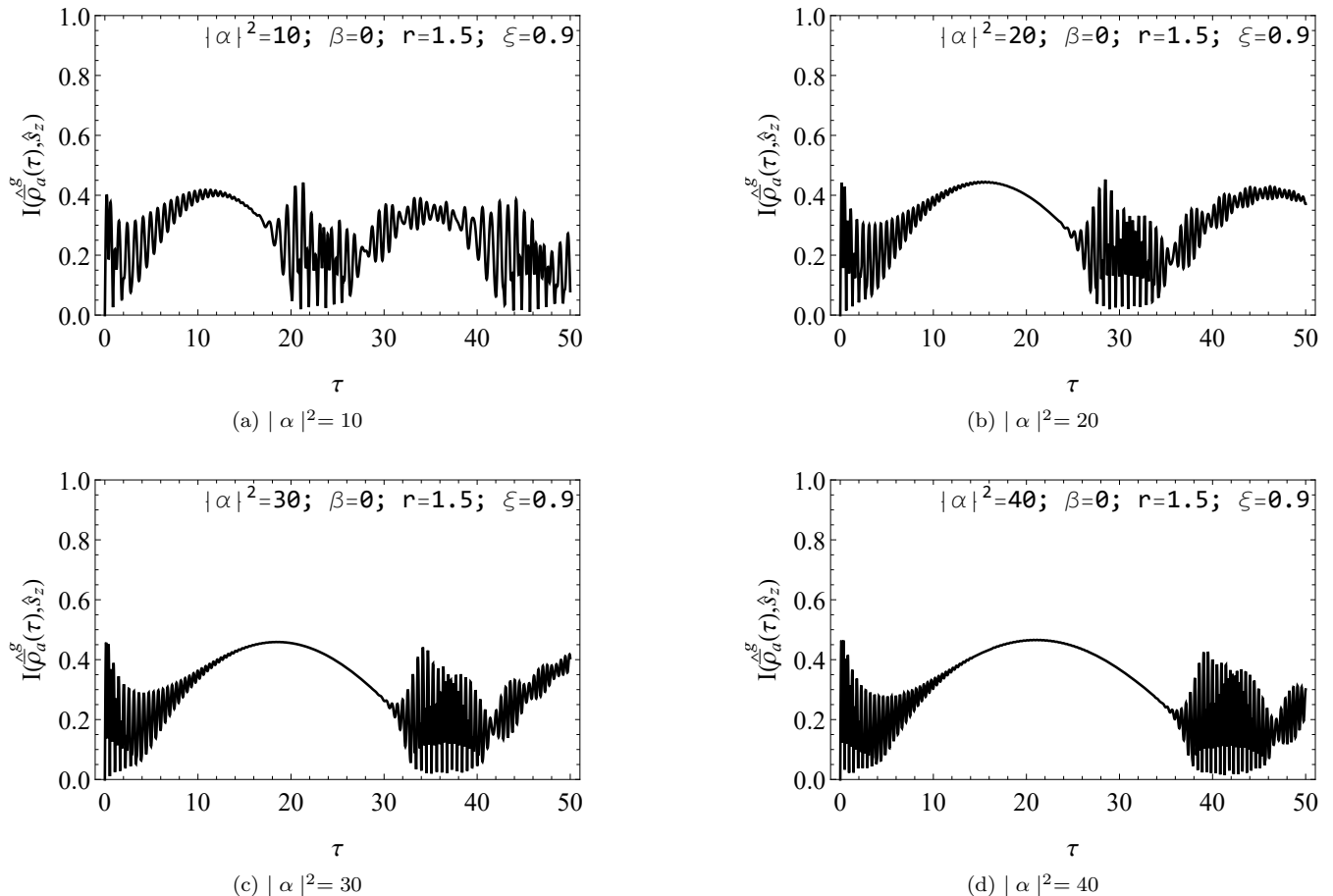


FIG. 2: Time evolution of Wigner-Yanase Skew Information $I(\hat{\rho}_a^g(\tau), \hat{s}_z)$ at $\bar{\delta} = 2\xi\lambda = 1.8\lambda$ ($\xi = 0.9$), $r = 1.5$: Fig. (2a), $|\alpha|^2 = 10$, Fig. (2b), $|\alpha|^2 = 20$, Fig. (2c), $|\alpha|^2 = 30$ and Fig. (2d), $|\alpha|^2 = 40$.

With reference to the plots in Fig. (2):

- (i) an increase in field intensity results in more rapid oscillations in $I(\cdot)$ as visualised in Figs. 2a, 2b, 2c, 2d in the order of increasing field intensity, $|\alpha|^2$;
- (ii) longer revival times, τ_R , in the time evolution of $I(\cdot)$ is evident in Fig. (2b) compared to Fig. (2a); Fig. (2c) in comparison to Figs. (2a), (2b); Fig. (2d) compared to Figs. (2a), (2b), (2c) again for every rise in mean photon number and;
- (iii) the weak coupling set at $\xi = 0.9$, is not affected by variation in mean photon number, i.e., it is not weakened further or made stronger. Notice the almost constant upward shift above the maximally mixed state limit, $I(\cdot) = 0$ [30] for all variations in $|\alpha|^2$.

3.3. Variation of squeeze parameter

We evaluate the Wigner-Yanase skew information in Eq. (8a) at fixed field intensity, $|\alpha|^2 = 30$, coupling strength, $\xi = 0.9$, difference frequency detuning, $\delta = 0, \beta = 0$ while varying upwards the squeeze parameter, $r = 0.5, 1, 1.5, 2$ and provide the corresponding plots in Figs. 3a, 3b, 3c and 3d.

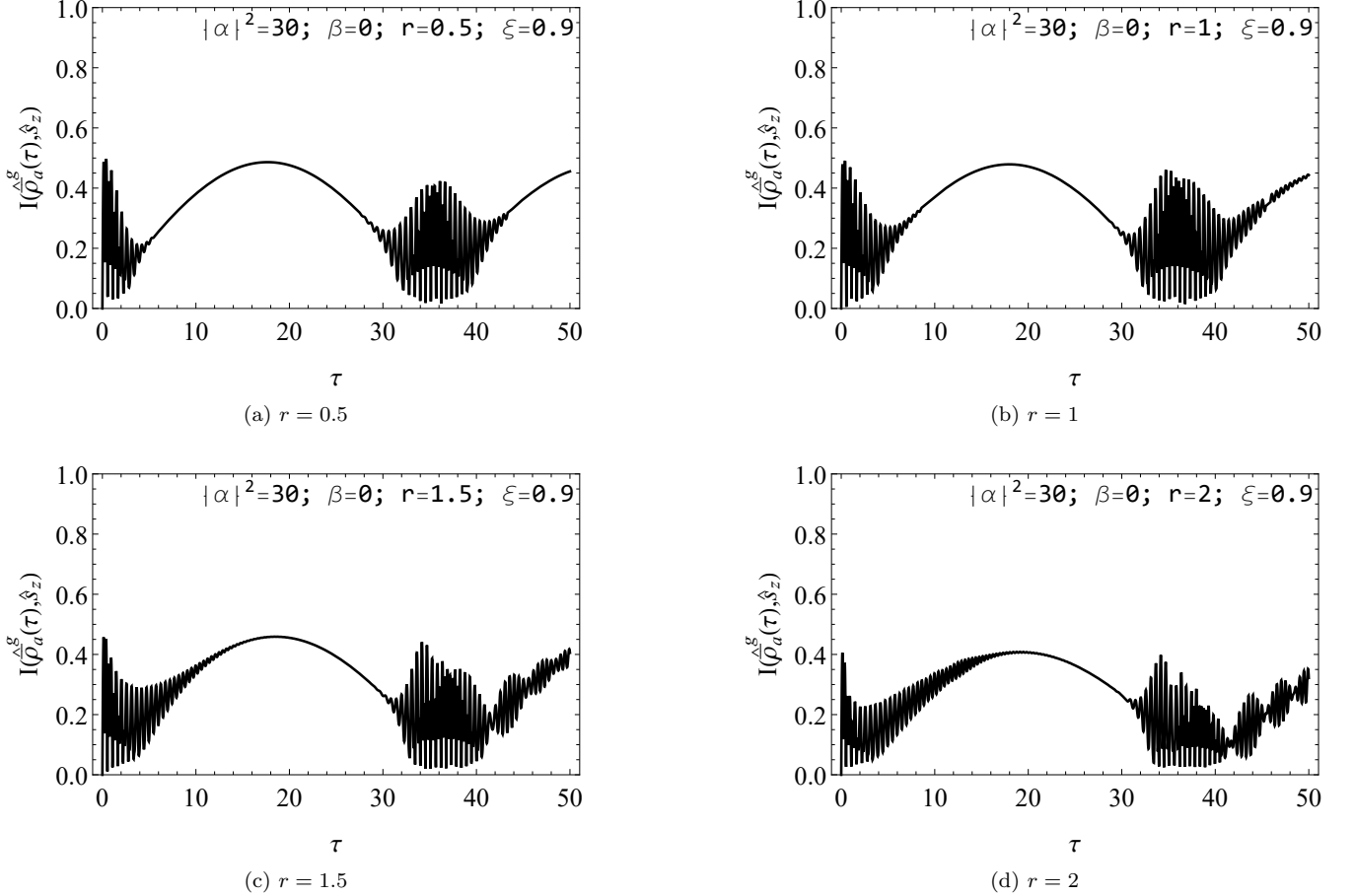


FIG. 3: Time evolution of Wigner-Yanase Skew Information $I(\hat{\rho}_a^g(\tau), \hat{s}_z)$ at $\bar{\delta} = 2\xi\lambda = 1.8\lambda$ ($\xi = 0.9$), $|\alpha|^2 = 30$: Fig. (3a), $r = 0.5$, Fig. (3b), $r = 1$, Fig. (3c), $r = 1.5$ and Fig. (3d), $r = 2$.

From the plots in Fig. 3, we conclude the following:

- (i) the effect of weak atom-field coupling $\xi = 0.9$ is evident, marked by a slight vertical shift in the time evolution of the Wigner-Yanase skew information above $I(\cdot) = 0$ in Figs. 3a, 3b, 3c, 3d and it is unaffected by upward variations in squeeze parameter, r ;
- (ii) in the example in Fig. 3a set at low squeeze parameter, $r = 0.5$, the evolution tends to attain the coherent pure state value, $I(\cdot) \simeq \frac{1}{2}$ [30, 42] at the middle of collapse of $W(\tau)$ (see example in Fig. 1a). Also notice that there is no ringing after the revival phase, $\tau > 40$ and;
- (iii) as the squeeze parameter is increased (see Figs. 3b, 3c, 3d), the oscillations in $I(\cdot)$ becomes more rapid, the peak value in $I(\cdot)$ reduces with every increase in r indicating diminished tendency of the atom-field states to evolve to pure state (see Figs. 3c, 3d) and ringing revivals [18, 23] are evident at $\tau > 40$.

4. CONCLUSION

In this study, we have analysed atomic non-classicality measured by the Wigner-Yanase skew information during the AJC interaction when an initial squeezed coherent field mode is considered. It is clear that reducing atom-field coupling, $\xi = \frac{\omega}{\lambda}$, which can also be viewed as an upward variation in sum frequency, $\bar{\delta} = 2\xi\lambda$, preserves the set field-mode squeezing for a longer period of time. The net effect as visualised in the provided examples, is delay in revival of atomic inversion coupled with a decrease in degree of entanglement, i.e., the atom-field states remain mixed as time develops and not maximally mixed. What is more, is that increasing the field intensity results in improved oscillations in the dynamics of the Wigner-Yanase skew information and a simultaneous delay in revival of atomic inversion. In this set-up, we see that for a fixed field-mode squeezing, r , upping the field intensity, the atom-field states tend to evolve to an approximate pure state, $I(\cdot) \simeq \frac{1}{2}$, at the middle of collapse of atomic population inversion similar to when a coherent field mode is considered [42]. This is because the coherent part, $|\alpha|^2$, of the squeezed coherent field-mode state dominates the squeezed part, $\sinh(r)$. The ringing revivals is however not affected as provided in the examples. Finally, when we increase the squeeze parameter, r , the oscillations in the temporal evolution of the Wigner-Yanase skew information become more rapid, occur in the mixed state range $0 < I(\cdot) < \frac{1}{2}$ and develop ringing revivals basically due to an increased number of squeezed photons in the coherent field.

ACKNOWLEDGEMENT

I thank Tom Mboya University in Kenya, for availing the required infrastructure to carry out this study.

DATA AVAILABILITY

All data required is available in this manuscript.

DISCLOSURE STATEMENT

The author declares no conflict of interest towards publication of this work.

NOTES ON CONTRIBUTORS

The author wrote and analysed each section of this manuscript as presented.

REFERENCES

- [1] Rabi, I.I., Phys. Rev. **49**, 324 (1936).
- [2] Rabi, I.I., Phys. Rev. **51**, 652 (1937).
- [3] Braak, D., Phys. Rev. Lett. **107**, 100401 (2011).
- [4] Braak, D., Chen, Q.-H., Batchelor, M.T., and Solano, E., J. Phys. A Math. Theor **49**, 300301 (2016).
- [5] Xie, Q., Zhong, H., Batchelor, M.T., and Lee, C., J. Phys. A Math. Theor. **50**, 113001 (2017).
- [6] Omolo, J.A., arXiv preprint [arXiv:2103.09546](https://arxiv.org/abs/2103.09546) (2021).
- [7] Mayero, C., Omolo, J.A., and Okeyo, O.S., Journal of Modern Physics **12**, 408 (2021).
- [8] Mayero, C. and Owiny, P., Quantum Physics Letters **10**, 23 (2021).
- [9] Jaynes, E.T. and Cummings, F.W., Proceedings of the IEEE **51**, 89 (1963).
- [10] Shore, B.W. and Knight, P.L., J. Mod. Opt. **40**, 1195 (1993).
- [11] Shore, B.W. and Knight, P.L., in *Physics and Probability : Essays in Honour of Edwin T. Jaynes*, edited by W. Grandy, Jr and P. Milonni (Cambridge University, Press, 1993), pp. 15–32.
- [12] Omolo, J.A., Preprint Research Gate, DOI:10.13140/RG.2.2.30936.80647 (2017).
- [13] Gerry, C. and Knight, P.L., *Introductory Quantum Optics* (Cambridge University Press, 2005).
- [14] Allen, L. and Eberly, J.H., *Optical resonance and two-level atoms*, vol. 28 (Courier Corporation, 1987).
- [15] Haroche, S., Rev. Mod. Phys. **85**, 1083 (2013).
- [16] Omolo, J. A., arXiv preprint [arXiv:2103.06577](https://arxiv.org/abs/2103.06577) (2021).
- [17] Mayero, C., Quantum Inf. Process **22**, 182 (2023).
- [18] Mayero, C. and Omolo, J. A., Quantum Inf. Process **23**, 1 (2024).
- [19] Loudon, R. and Knight, P.L., J. Mod. Opt. **34**, 709 (1987).

- [20] Knight, P. L. and Bužek, V., in *Quantum Squeezing*, edited by Drummond, P.D. and Ficek, Z. (Springer Berlin Heidelberg, Berlin, Heidelberg, 2004), pp. 3–32.
- [21] Mandel, L., *Phys. Scripta* **1986**, 34 (1986).
- [22] Zaheer, K. and Zubairy, M.S. (New York: Academic Press, 1987), vol. 28, p. 143.
- [23] Moya-Cessa, H. and Vidiella-Barranco, A., *J. Mod. Opt.* **39**, 2481 (1992).
- [24] Milburn, G.J., *Optica Acta: Int.J.Opt.* **31**, 671 (1984).
- [25] Satyanarayana, M.V., Rice, P., Vyas, R., and Carmichael, H.J., *JOSA B* **6**, 228 (1989).
- [26] Schleich, W. and Wheeler, J.A., *JOSA B* **4**, 1715 (1987).
- [27] Schleich, W., Walls, D.F., and Wheeler, J.A., *Phys. Rev. A* **38**, 1177 (1988).
- [28] Teich, M.C. and Saleh, B.E.A., *Quant. Opt.* **1**, 153 (1989).
- [29] Wigner, E. P. and Yanase, M. M., *Proc. Natl. Acad. Sci.* **49**, 910 (1963).
- [30] Dai, H. and Luo, S., *Phys. Rev. A* **100**, 062114 (2019).
- [31] Forn-Díaz, P., Lisenfeld, J., Marcos, D., Garcia-Ripoll, J., Solano, E., Harmans, C.J.P.M., and Mooij, J.E., *Phys. Rev. Lett.* **105**, 237001 (2010).
- [32] Pradhan, P., Cardoso, G.C., Morzinski, J., and Shahriar, M.S., arXiv preprint [quant-ph/0402122](https://arxiv.org/abs/quant-ph/0402122) (2004).
- [33] Cardoso, G.C., Pradhan, P., Morzinski, J., and Shahriar, M.S., *Phys. Rev. A* **71**, 063408 (2005).
- [34] Scully, M.O., Zubairy, M.S., et al., *Quantum Optics* (Cambridge University Press, 1997).
- [35] Jaeger, G., *Entanglement, information, and the interpretation of quantum mechanics* (Springer Science & Business Media, 2009).
- [36] Nielsen, M.A. and Chuang, I.L., *Quantum Computation and Quantum Information* (Cambridge University Press, 2011).
- [37] Enriquez-Flores, M. and Rosas-Ortiz, O., in *AIP Conference Proceedings* (American Institute of Physics, 2010), vol. 1287, pp. 74–79.
- [38] G. Alber, T. Beth, M. Horodecki, P. Horodecki, R. Horodecki, M. Rötteler, H. Weinfurter, R. Werner, and A. Zeilinger, *Quantum information: An introduction to basic theoretical concepts and experiments*, vol. 173 (Springer, 2003).
- [39] P. Kaye, R. Laflamme, M. Mosca, et al., *An introduction to quantum computing* (Oxford university press, 2007).
- [40] Gea-Banacloche, J., *Phys. Rev. Lett.* **65**, 3385 (1990).
- [41] SUBEESH, T., SUDHIR, V., AHMED, A.B.M., and SATYANARAYANA, M.V., *Nonlinear Opt. Quantum Opt.* **44** (2012).
- [42] Dai, H., Fu, S., and Luo, S., *Phys. Lett. A* **384**, 126371 (2020).